One step beyond: Different step-to-step transitions exist during continuous contact brachiation in siamangs

Fana Michilsens[1,2,*], Kristiaan D'Août[1,2], Evie E. Vereecke[1,3] and Peter Aerts[1,4]

[1]Department of Biology, University of Antwerp, CDE-C, Universiteitsplein 1, 2610 Wilrijk, Belgium
[2]Centre for Research and Conservation, RZSA, Kongingin Astridplein 26, 2018 Antwerp, Belgium
[3]Biomedical Science Group Kulak, University of Leuven, Etienne Sabbelaan 53, 8500 Kortrijk, Belgium
[4]Department of Movement and Sport Sciences, University of Ghent, Watersportlaan 2, 9000 Ghent, Belgium
*Author for correspondence (fana.michilsens@ua.ac.be)

Biology Open 1, 411–421
doi: 10.1242/bio.2012588

Summary

In brachiation, two main gaits are distinguished, ricochetal brachiation and continuous contact brachiation. During ricochetal brachiation, a flight phase exists and the body centre of mass (bCOM) describes a parabolic trajectory. For continuous contact brachiation, where at least one hand is always in contact with the substrate, we showed in an earlier paper that four step-to-step transition types occur. We referred to these as a 'point', a 'loop', a 'backward pendulum' and a 'parabolic' transition. Only the first two transition types have previously been mentioned in the existing literature on gibbon brachiation. In the current study, we used three-dimensional video and force analysis to describe and characterize these four step-to-step transition types. Results show that, although individual preference occurs, the brachiation strides characterized by each transition type are mainly associated with speed. Yet, these four transitions seem to form a continuum rather than four distinct types. Energy recovery and collision fraction are used as estimators of mechanical efficiency of brachiation and, remarkably, these parameters do not differ between strides with different transition types. All strides show high energy recoveries (mean =70±11.4%) and low collision fractions (mean =0.2±0.13), regardless of the step-to-step transition type used. We conclude that siamangs have efficient means of modifying locomotor speed during continuous contact brachiation by choosing particular step-to-step transition types, which all minimize collision fraction and enhance energy recovery.

Key words: Hylobatidae, Suspensory locomotion, External work, Energy recovery

Introduction

When studying brachiation, two gait types can be distinguished based on spatiotemporal characteristics (Fleagle, 1976; Bertram et al., 1999). Brachiation at a low forward velocity mostly results in continuous contact brachiation, where at least one hand is always in contact with the substrate and often a double contact phase (i.e. both hands contacting the substrate) is present. Higher forward velocities result mostly in ricochetal brachiation, with a flight phase (no hand contact) between consecutive handholds. However, from a mechanical perspective, based on dynamics and considering the centre of mass of the entire body (bCOM) during a brachiation sequence, more than two bCOM patterns can be distinguished. During a previous study (Michilsens et al., 2011), we observed four different step-to-step transition types based on the path of the bCOM. More specifically, during continuous contact brachiation, transfer between handholds can occur using a 'point' transition (Fig.1a), a 'loop' transition (Fig. 1b) or even a 'backward pendulum' movement can be used (Fig. 1c). Occasionally, a 'parabolic' transition (Fig. 1d) is observed during double contact phase, the transition type typical for (the flight phase in) ricochetal brachiation.

A point transition is considered the optimal transition type for continuous contact brachiation (Bertram et al., 1999). Here, each swing phase starts and ends when the bCOM is at its highest and the velocity is zero at the instant of double contact. When the velocity is not zero at the beginning and end of the swing phase and handholds are placed further apart (more than 1.2 m), ricochetal brachiation occurs (Bertram et al., 1999; Bertram and Chang, 2001). In those cases, a flight phase is present where the bCOM describes a parabolic trajectory (Bertram et al., 1999). This parabolic phase, however, seems to be possible during short double hand contact as well (Fig. 1d), although it has never been described as such. On the other hand, when handholds are placed closer together in a way that is not optimal for the animal (e.g. shorter than two times forelimb length), a loop transition is described as a way for the animal to begin the next support phase with a fully extended support arm (Chang et al., 1997). However, the backward pendulum, where the bCOM actually moves backwards and describes a new, shorter pendulum path during double hand contact, has never been described for gibbon brachiation, except by Michilsens et al. (Michilsens et al., 2011). Moreover, the fact that these different transition types are

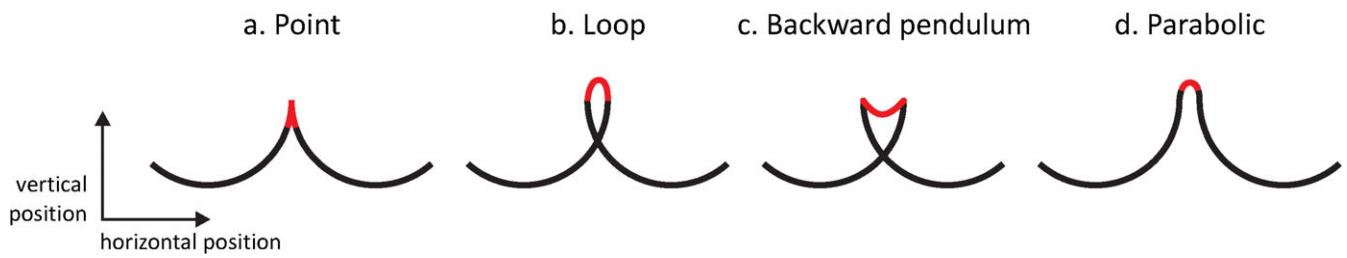

Fig. 1. Schematic drawing of the (spatial) bCOM trajectory associated with different transition types used in continuous contact brachiation. a) point; **b)** loop; **c)** backward pendulum and **d)** parabolic. Red colour refers to double hand contact, black to single hand support.

observed in the same animal on the same setup is highly intriguing.

The central aim of this paper is to characterize the various step-to-step transition types during continuous contact brachiation, both kinematically and kinetically. We expect that the brachiation strides characterized by the different step-to-step transition types will show different dynamics, which we can investigate using four main hypotheses.

(1) First hypothesis: The four transition types can be distinguished by different joint angle profiles and by different substrate reaction forces. Joint angles and substrate reaction forces will be used to describe the relation between bCOM kinetics and the kinematics of two relevant joints, i.e. shoulder and elbow, in the different transition types.

(2) Second hypothesis: Brachiation strides with different step-to-step-transition types may imply different costs. 3D video analyses enable us to estimate which mechanisms are used to reduce the external work during brachiation and transition in absence of metabolic cost measurements due to restrictions inherent to working with untrained zoo animals. Mechanical costs (also translating to metabolic costs) of brachiation will on the one hand, largely depend upon the amount of energy exchange during the pendular swing (Cavagna et al., 1976) and, on the other hand, on the amount of energy lost during the transitions from one step to the next (Bertram et al., 1999; Usherwood and Bertram, 2003). Therefore, energy recovery (ER) and collision fraction (CF) are used as estimators for the mechanical efficiency of the brachiation movements as these both express (irrespective the absolute amount) the fractional reduction of the work that has to be done on the bCOM. ER is calculated as a measure of the amount of energy that can be recovered passively by using a pendular movement, whereas CF, as proposed by Lee et al. (Lee et al., 2011), is a measure for efficiency of collision avoidance. Both ER and CF have values between 0 and 1. The higher the ER, the more kinetic and potential energy are converted into each other and less work is necessary to keep the bCOM going. The CF is the actual collision relative to the potential collision (Lee et al., 2011), thus indicating how much collision reduction actually occurs in the observed brachiation sequences. The lower the CF, the more collision reduction there is, implying that the motion is adjusted and a mechanism is used to decrease the actual collision. Therefore, less energy will be lost than predicted by collisional theory. The amount of energy that is saved or lost during collision, however, cannot yet be determined at this point. The difference in ER and CF between the brachiation strides with different transition types will be determined to evaluate if certain transition types imply a more efficient use of the external work. Given that a higher ER and lower CF presumably imply less mechanical costs at the level of the bCOM (i.e. external work), an association which is valid unless internal work due to intermembral displacements is raised proportionally.

(3) Third hypothesis: If brachiation strides with different transition types imply different costs, the experience of the animal may induce a preference for the transition type with the lowest cost. Three individuals are used in this study and the individual preference for a specific type of transition will be tested. This individual preference may be based on age, experience or body size effect.

(4) Fourth hypothesis: Locomotion speed will differ between the strides with different transition types. In a previous publication (Michilsens et al., 2011), we showed that ER decreases with speed and that the different bCOM patterns could explain this effect. A faster brachiating siamang has a lower energy recovery and this could be caused by using a transition type with a less efficient energy exchange mechanism. Following this hypothesis, each transition type should be used during strides with different speeds and strides with different transition types should entail different costs (cfr. H2).

Materials and Methods

The experimental design, setup and analysis were largely similar to those used and described in a previous publication (Michilsens et al., 2011). Below we explain briefly how data collection and analysis were executed in this study. For a more detailed description we refer to our previous publication (Michilsens et al., 2011).

Subjects

We recorded data of a family of three siamangs (*Symphalangus syndactylus*; Fam. Hylobatidae) during voluntary brachiation in their outdoor enclosure in Antwerp Zoo (Royal Zoological Society Antwerp, Belgium). Subject data can be found in Table 1. All individuals were in excellent health, demonstrated no musculoskeletal or other pathologies and showed no obvious aberration in locomotion (e.g. no "limping"). An operant conditioning method (clicker training) was used to encourage the animals to brachiate over the setup. When brachiation was used over the entire setup, the animals were rewarded with a click and a food reward. This motivated the animals to brachiate back and forth over the instrumented setup, yet all locomotor bouts remained spontaneous and were executed at a self-chosen speed, gait or transition type.

Setups

A steel beam of 7 meters was installed in the outdoor animal enclosure and handholds were placed below this beam. Two setups were used:

Setup 1: Eight handholds placed perpendicular to the direction of movement, at intervals of 80 cm and aligned in the horizontal plane; hence step lengths are fixed at 80 cm or a multiple thereof. The three middle handholds are equipped with force transducers (see setup 2 in a previous publication) (Michilsens et al., 2011).

Fig. 2. Detail of Kistler force transducer installed in setup 2.

Setup 2: Five handholds placed perpendicular to the direction of movement at intervals of 120 cm and aligned in the horizontal plane; hence step lengths are fixed at 120 cm or a multiple thereof. The three middle handholds are equipped with force transducers (Fig. 2).

The first setup was used as the main setup for data collection. The second setup, initially used for a different purpose, offered us extra information on continuous contact brachiation at higher velocities.

Four cameras operating at 50 fields per second were installed around the steel beam and recorded the movements of the siamangs from four different angles simultaneously. The four cameras were synchronized and calibration was carried out by recording a calibration cube with exactly known dimensions (0.5 m* 0.5 m* 0.5 m) hanging parallel to the steel beam between the two middle handholds prior to each recording session. Only strides passing through the calibrated volume (i.e. on the three middle handholds) were analyzed and the handholds before and after that are considered as take-off and ending zones to guarantee a continuous motion within the measuring volume. Digitization of the handholds in the periphery (of which we know the exact measures) showed only a small measuring error (≤10%) when compared with the actual dimensions of the handholds.

Data were collected over a period of 4 months. A recording session lasting 30 minutes took place once a week. The animals were free to choose their locomotor velocity and brachiation type. During the first couple of weeks, the animals were habituated to the setup and only video recordings were made (no force transducers installed). A sequence was considered as continuous contact brachiation (CCB) and suitable for analysis when there was at least one double hand support phase and the animal made a continuous progress over the entire setup without using the feet for extra support or without pausing in-between. Considering it is voluntary brachiation, the bouts include some acceleration and deceleration and are in general not steady state.

Video analyses

For each individual and each setup, we aimed to digitize at least three sequences of CCB for which substrate reaction forces were also available. However, for subject E only two sequences were digitized (Table 1) as he only occasionally used CCB prior to installation of the force transducers, and completely stopped using CCB after installation of the force transducers. Subject G never used CCB on setup 2, so no data could be included in the analysis for that setup. Additional sequences, where either only video recordings or substrate reaction forces were collected due to technical issues, were included in the final analysis. The sequences were randomly selected from various recording days and without a priori knowledge of locomotor speed. A total of 21 sequences were included in the analysis (incl. 9 with both force and video data). A sequence is defined as a recording of the animal brachiating from one end of the instrumented setup to the other.

Video images were digitized manually frame by frame for each camera view using Kwon visual 3D (Visol, Inc; Kyonggi-do, Korea). Zoo policy does not allow any direct interaction with the animals, excluding the use of segmental-markers for kinematical analysis. However, repeatability (from three observers digitizing the same sequence) on the 3D coordinates of shoulders and hip was tested and resulted in a value of 95% on average. 21 landmarks were defined: crown, nose, chin, shoulders, elbows, wrists, metacarpals, fingertips, hips, knees, heels and toes (right and left where possible). This resulted in a 3D 16-linked-segment body model consisting of the following segments: head, trunk, upper arm, lower arm, hand, fingers, upper leg, lower leg and foot (left and right where possible). The raw positional data were filtered using a 4th order Butterworth Low-Pass filter with a cut-off frequency based on the residual plot (± 6 Hz). Entire sequences were digitized, but further analysis was carried out for one stride per sequence. A stride is defined as the period from one hand contact until the same hand made contact with a support again

Body-segment parameters were obtained during dissections of four siamang cadavers (see our previous publications for more details on these subjects (Michilsens et al., 2009) and for measured values (Michilsens et al., 2011)) and include segment mass normalized to total body weight, positions of the segment centre of mass and moments of inertia normalized to respective segment length. These relative body-segment parameters are used to calculate the instantaneous three dimensional position of the entire body centre of mass (bCOM). Joint angles as well as the instantaneous velocity of the bCOM were derived. From the position and velocity of the bCOM derived from kinematic data, the potential and kinetic energy of the body were calculated throughout the sequence using the following formulae:

$$E_K = 0.5 * m * \left(v_x^2 + v_y^2 + v_z^2\right) \quad (1)$$

$$E_p = m * g * h \quad (2)$$

Where E_K is translational kinetic energy (J), E_p is gravitational potential energy (J), m is the mass of the individual (kg), v_x, v_y and v_z are the lateral, forward and

Table 1. Subject data and number of analyzed sequences. "Total analysis" includes analysis of both video recordings and force data. For some sequences, forces were not measured but 3D video-analysis was executed ("Video only"). For some sequences, forces were recorded but video analysis was impossible, due to technical issues ("Force only").

Individual	Sex	Age (years)	Age category	Mass (kg)	Total analysis Setup1/2	Force only	Video only
H	Male	37	Adult	12.5	3/3	3	3
E	Male	6	Subadult	11	0	0	2
G	Female	3	Juvenile	7.5	3	1	3
All subjects	-	-	-	-	6/3	4	8

vertical instantaneous velocities (m/s) and h is the vertical position of the bCOM relative to the reference frame (m).

Shoulder and elbow joint angles

Shoulder angles are calculated as the joint angle between trunk and upper arm, and elbow angles as the joint angle between lower and upper arm. Instantaneous joint angles are presented in degrees relative to stride duration. Shoulder angles are considered 0° when the upper arms hang down along the trunk, and 180° when raised entirely above the head. Elbow angles reach 0° when (theoretically) completely flexed and 180° when fully extended.

Substrate reaction forces

Three force transducers (Kistler Holding AG; Winterthur, Switzerland) were used to measure substrate reaction forces in all three directions (x lateral, y longitudinal and z vertical). Only longitudinal (fore-aft, Fy) and vertical forces (Fz) were used for analysis. Each force transducer was connected to an amplifier and data were read into the computer as volts. A custom-written Labview program (version 2009, National Instruments; Austin, Texas, USA) was used to collect (1000 Hz), calibrate and filter the data.

Calibration was done by hanging a mass of exactly 8 kg to the handhold, either directly (for vertical calibration) or via a pulley around another handhold at the same level (for horizontal calibration). A cut-off frequency of 20 Hz was applied before exporting the data to Microsoft Excel 2007 for further analysis. For each support phase the vertical peak force was extracted and divided by body weight to allow for comparison between individuals (relative maximal vertical reaction force = rel Fz max; expressed as the number of times bodyweight). Reaction force patterns over a stride and relative vertical peak forces were compared between transition types of CCB.

Reference frame

For both the kinematics and the substrate reaction forces, the same 3D reference grid was used with a vertical Z-axis pointing upwards and two perpendicular horizontal axes (X and Y axes). Upward forces acting from the handhold on the animal are positive. The direction of brachiation determines the sense of the longitudinal horizontal (Y) axis. As such, positive substrate reaction forces in the longitudinal direction (Y-axis) accelerate the animal in the direction of motion.

Energy recovery

Percent mechanical energy recovery (ER) is a measure for the amount of the energy exchange between potential and kinetic energy of the bCOM (Cavagna et al., 1976). The ER was determined the same way as in a previous publication (Michilsens et al., 2011):

$$ER = \frac{\left(\sum \Delta^{+} E_P + \sum \Delta^{+} E_K\right) - \sum \Delta^{+} E_{tot}}{\left(\sum \Delta^{+} E_P + \sum \Delta^{+} E_K\right)} * 100 \quad (3)$$

Where $\Sigma\Delta^{+}$ is the sum of the positive increments of energy (i.e. the increases in energy over each time-step of 0.02 s), E_p is gravitational potential energy (J), E_K is translational kinetic energy (J) and E_{tot} is the sum of E_p and E_k, resulting in the total mechanical energy (J) (Bertram and Chang, 2001). In phase fluctuation of E_p and E_k will result in low ER (low energy exchange), whereas out-of-phase fluctuation of E_p and E_k will result in high ER (high energy exchange).

Energy recovery was calculated for each complete stride in each sequence from which bCOM position and velocity were available. Only kinematic data were used to calculate ER. A stride was determined as the period from one hand contact until the same hand made contact with the support again.

Collision fraction

Collision fraction is proposed by Lee et al. (Lee et al., 2011) as a measure for collision reduction. It is calculated as follows:

$$CF = \Phi / (\hat{\lambda} + \Theta) \quad (4)$$

Where Φ is the collision angle (angle between substrate force vector and bCOM velocity vector, shifted by $\pi/2$) in radians averaged over the stride, $\hat{\lambda}$ is the velocity angle in radians averaged over the stride and Θ is the force angle in radians averaged over the stride. Velocity angles were calculated from the velocity vectors deduced from the kinematic data (by deriving the positional data of the bCOM over time). Force angles were calculated from the resultant force vector of the measured substrate reaction forces.

Collision fraction results in a number between zero and one. As suggested by Lee et al. (Lee et al., 2011), a CF of zero is an idealized situation where force and velocity vectors remain perpendicular to each other throughout the stride. In this case, mechanisms are present to reduce collisions and thus collisional losses. A CF of one indicates a compliant spring loaded (inverted) pendulum, where the force and velocity vectors result in a non-perpendicular position relative to each other. In this case, no collision reduction is present and collisional losses may occur.

Locomotor speed

To correct for differences in body size of the animals, the square root of Froude number was taken as dimensionless measure of locomotor speed (Vaughan and O'Malley, 2005). Dimensionless speed (v_d) was calculated as:

$$V_d = \langle V \rangle \Big/ \left(\sqrt{(1 * g)}\right) \quad (5)$$

Where $<v>$ is the average forward velocity of the bCOM during one stride (m/s), l is a characteristic linear dimension of the animal (m) and g is the gravitational constant (m/s^2).

Additionally, the percentage of double hand contact (%DHC) was calculated as the duration of double hand contact during the transition divided by the entire stride duration. %DHC is correlated with speed.

Statistics

A Fisher exact test was used to determine individual preference for transition type. Using separate ANOVA models, we tested whether individual, transition type, setup and speed (including their two-way interactions) affected ER, %DHC, rel Fzmax, and CF. Interactions between ER, CF and %DHC, and between vertical peak force and speed, were tested using Pearson correlations. All tests were executed in SAS 9.2 for Windows (SAS Institute Inc. Cary, NC, USA). Normality of the data and residuals was tested with a Shapiro-Wilk test. All parameters demonstrated a W-value above 0.9 and were, therefore, considered normally distributed. For all results p-values lower than 0.05 were considered significant.

Results

Characterization of the different transition types (Hypothesis1)

For each brachiation stride with one of the observed step-to-step-transition types an example stride is presented and joint angles, bCOM velocities and substrate reaction forces are described. The leading arm is defined as the arm grabbing the second handhold (initiating double contact) and the trailing arm is the arm holding the first handhold (ending the double contact after release). Shoulder angles presented are 3D joint angles, therefore we refer to increasing and decreasing angles to address the position of the upper arm relative to the trunk. Note that horizontal substrate reaction forces refer to the longitudinal forces (Fy).

Pendular transition (Fig. 3a–d)

The trailing arm elbow extends during double contact and the shoulder angle decreases slightly. Simultaneously, a negative horizontal substrate reaction force (-Fy) is measured at the first handhold and the body moves backward. At the other handhold, the leading arm is already extended when double hand contact occurs and extends further during double contact, while a positive horizontal substrate reaction force (+Fy) is measured. These measurements imply that the trailing and leading arm work together to, respectively, pull and push the body backwards. During double contact, the total horizontal force remains close to zero, implying a nearly constant velocity, at which the body moves backward (velocity is negative) (Fig. 3c).

The vertical forces (Fz) are almost equally divided over both handholds during the entire double contact phase. In the beginning of double contact, a peak vertical force is reached due to the active deceleration of the downwards moving body. A negative vertical velocity is measured at this point. At the end of double hand contact, another peak occurs, this time caused by an upward acceleration.

Loop transition (Fig. 3e–h)

The trailing arm flexes from the second half of the first swing phase onwards and during double contact. Simultaneously, a

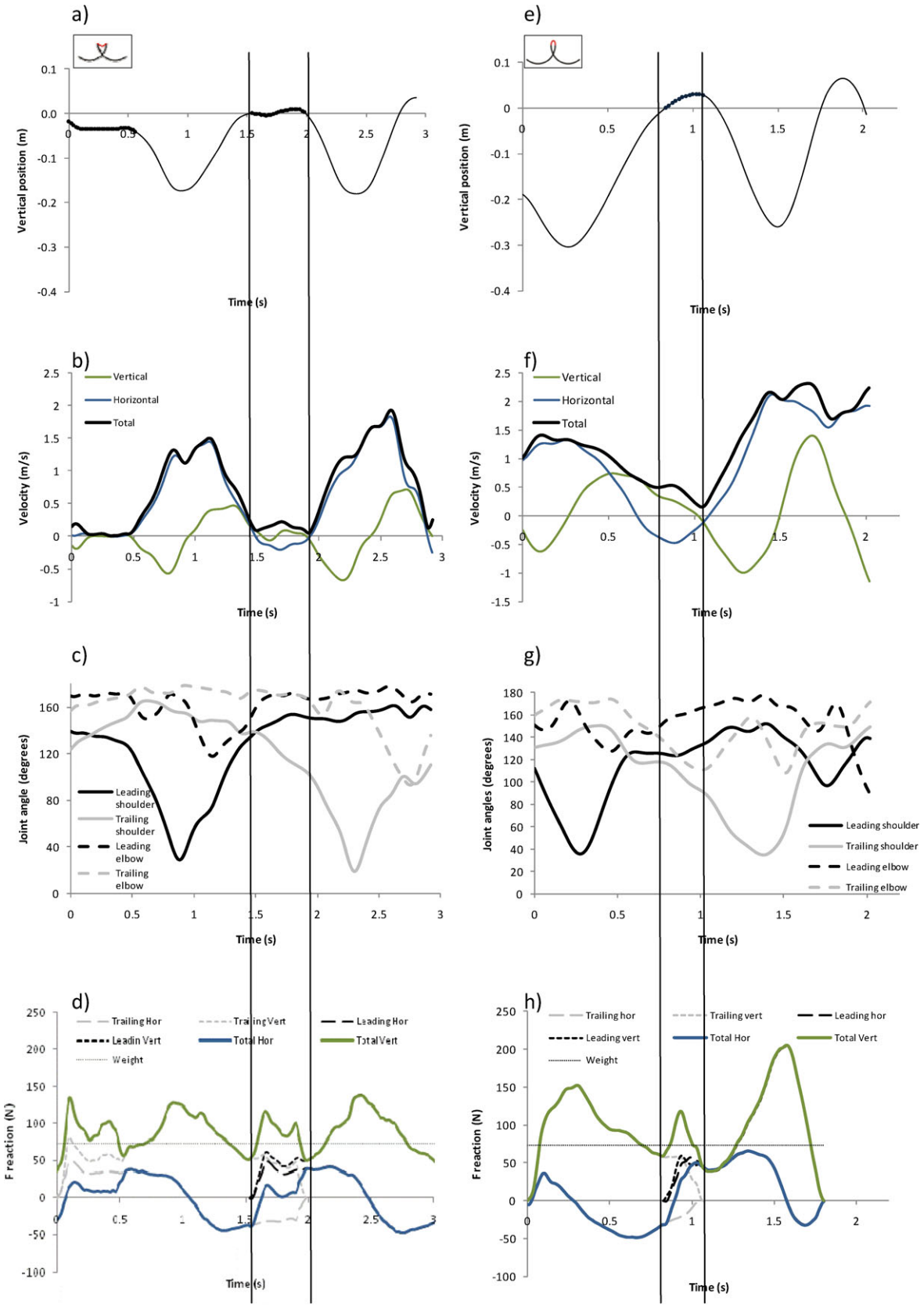

Fig. 3. Example files for the pendular transition (left a–d) and the loop transition (right e–h). With **a)** and **e)** bCOM vertical position; height is zero at the start of double contact, **b)** and **f)** instantaneous velocity, **c)** and **g)** shoulder and elbow angles and **d)** and **h)** handhold reaction force presented over the time of one stride. The leading arm is defined as the arm grabbing the second handhold (initiating double contact) and the trailing arm is the arm holding the first handhold (ending double contact at release). The horizontal dotted line in the force graphs indicates the bodyweight of the animal.

negative horizontal substrate reaction force (-Fy) is measured at the first handhold and the body moves back- and upwards. At the other handhold, the leading arm extends only slightly during the double hand contact and a positive horizontal substrate reaction force (+Fy) is measured which pushes the body backwards. The total horizontal substrate reaction force increases quickly and is positive during most of the double contact phase. Because the body is moving backward, this implies a decelerating movement against the general direction of movement. The vertical force (Fz) is gradually transferred from the trailing to the leading arm. Vertical force decreases in the trailing arm, while it increases in the leading arm. This results in one peak caused by an upward deceleration, before the body swings for- and downward again and the trailing arm is released.

Point transition (Fig. 4a–d)

Both shoulder angle and elbow angle from the trailing arm decrease only slightly during the swing and double contact phase, but the elbow flexes significantly at the end of double support. The negative horizontal substrate reaction force (-Fy) on the first handholds decreases quickly to zero, while the horizontal force on the second handhold increases rapidly, causing a peak horizontal force (+Fy) immediately before the end of the double contact. The leading arm shoulder angle and elbow angle are maximal during this phase. During both swing phases, the elbows of the non-supporting forelimbs are flexed, while the shoulders angles are maximal, which is in contrast with the pendular and loop transition sequences. The horizontal velocity remains positive during the entire stride, meaning the animal continuously moves forward. The peak in horizontal force coincides with a small peak in vertical force (Fz), caused by a short downward deceleration, quickly followed by a small downward acceleration.

Parabolic transition (Fig. 4e–h)

During the parabolic transition, only a very short period of double contact exists (accounting for only 3% of the stride). The trailing arm and the leading shoulder angles decrease, while the leading arm elbow slightly extends. However, both leading and trailing arm are more flexed in comparison with the point transition. Both horizontal (Fy) and vertical reaction forces (Fz) approach zero during double contact, indicating that hardly any force is exerted on the handholds and the body approaches a flight phase.

How do the different transition types differ dynamically?

Forces (Hypothesis 1)

The relative maximal vertical reaction force does not differ between transition types ($p=0.05$). However, the significance level is approached very closely and, when running a post hoc test, a significant difference is found between a loop and a pendulum transition, with the loop having a higher relative Fz max (1.75 times bodyweight compared to 1.60 times bodyweight, respectively). Parabolic and point transitions show an intermediate relative Fz max (1.70 times bodyweight).

A clear correlation is found between the relative maximal force and the speed ($p=0.02$), but no interaction effects are found. The effect of speed on maximal force is the same for each animal and each transition type.

Efficiency of brachiation mechanisms: ER and CF (Hypothesis 2)

ER and CF do not differ significantly between strides with different transition types ($p=0.13$ and $p=0.18$, respectively) (Fig. 5). The average ER ± s.d. (over all types and individuals) equal $69.7\pm11.4\%$ and CF 0.22 ± 0.127. In the calculations of the CF, there is one outlier. If this value is removed from the dataset, the average CF and s.d. are 0.186 ± 0.063. No correlation is found between ER and CF ($p=0.18$).

Individual preference (Hypothesis 3)

A Fisher exact test showed that there was no equal distribution of transition types over the individuals ($p=0.01$) (Fig. 6). The occurrence of transition types between individuals was significantly different, meaning there is an individual preference for a specific transition type. To take this into account with further testing, individual was added as a random factor.

Fig. 5 shows that subject H uses the pendulum transition the most and the parabolic transition the least; whereas it is the other way around for subject G. Subject E only uses parabolic and point transitions during our measurements.

Locomotor speed (Hypothesis 4)

Percentage of double hand contact differs ($p=0.0001$) between strides with different transition types, more specifically between the pendular and loop transition on the one hand and point and parabolic transition on the other ($p\leq0.03$) (Fig. 7). No effect of individual or setup is found, although individual is corrected for in a random statement. The pendular and loop transitions occur when the percentage of double hand contact is longest: on average 16% and 12% of the stride duration (no significant difference between these two types; $p=0.5$). When the percentage of double hand contact is low, a point or parabolic transition occurs (4% and 1% respectively, but no significant difference between these two types either; $p=0.7$).

Speed differs between the two setups, with the second one (handholds further apart) resulting in a higher speed (Fig. 7). However, because we are not interested in the difference between the setups, but want to correct for this difference, setup is added as a random statement in the model.

No interaction effect was found between type and individual ($p=0.2$), but both individual and transition type affect speed. The individual animals brachiated at different average speeds ($p=0.04$).

The speed used during the different transition types differs significantly ($p=0.01$) (Fig. 7). A post hoc test showed that actually only the pendular transition is used at significantly slower speeds than any other transition type. The average speed during a pendular transition is 0.32 and does not differ from the average speeds during a loop transition (0.39; $p=0.06$). Yet, the speed during a point transition and parabolic transition is significantly higher (0.42; $p=0.02$ and 0.44; $p=0.01$, respectively).

Percent of double hand contact and speed are negatively correlated (slope $=-0.73$; $p=0.0002$): when speed increases, %DHC decreases.

Discussion

From the hypotheses proposed in the introduction, the first hypothesis, i.e. that step-to-step transitions in continuous contact brachiation are characterized by differences in joint angles and

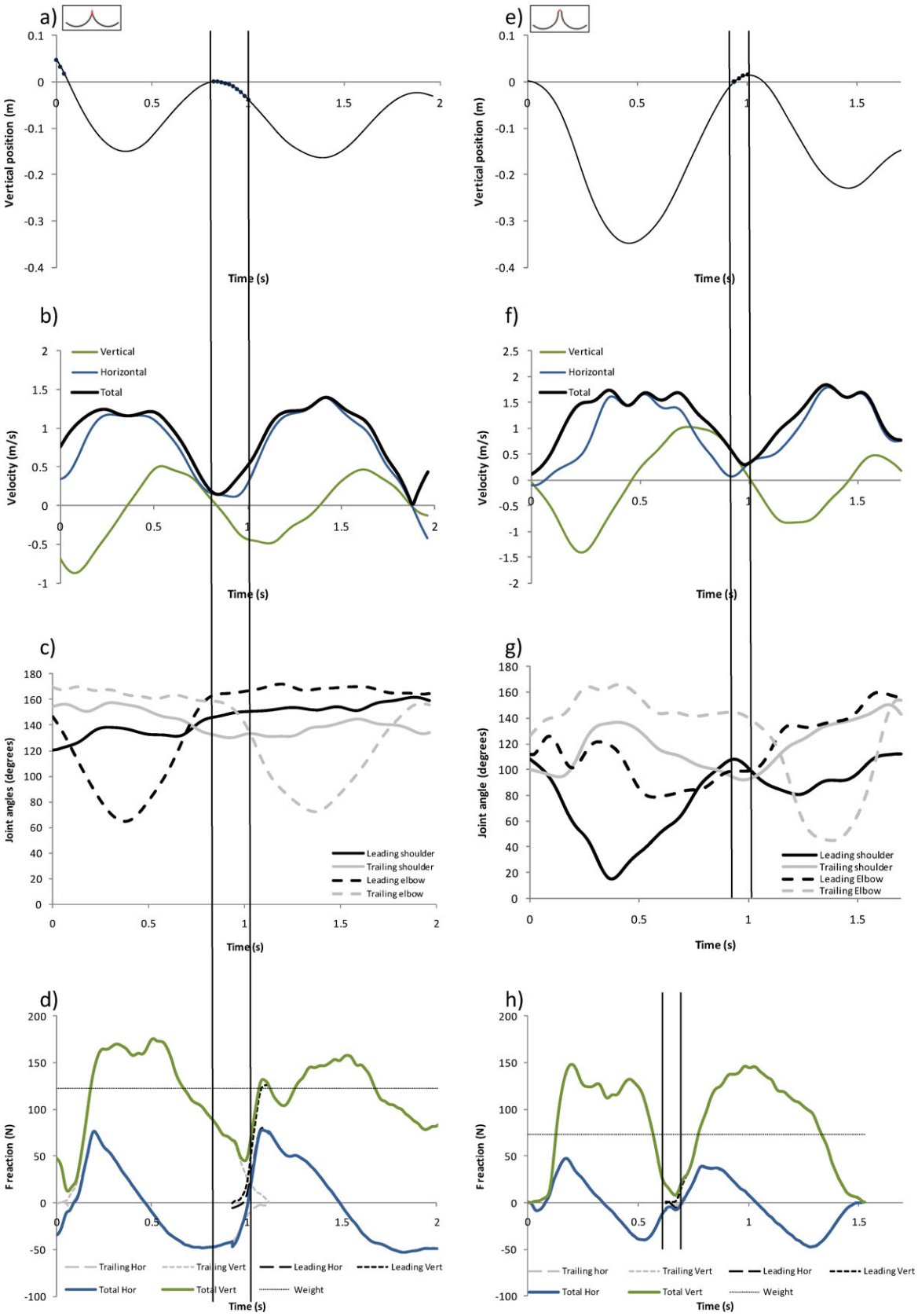

Fig. 4. Example files for the point transition (left a–d) and the parabolic transition (right e–h). With **a)** and **e)** bCOM vertical position; height is zero at the start of double contact, **b)** and **f)** instantaneous velocity, **c)** and **g)** shoulder and elbow angles and **d)** and **h)** handhold reaction force presented over the time of one stride. The forces displayed from the parabolic transition are from another sequence than the other graphs from this transition, because no total analysis was present for this transition type. Both presented sequences have a similar percentage of double hand contact (0.03 and 0.04), although the forces are from a faster sequence (0.47 to 0.37). The leading arm is defined as the arm grabbing the second handhold (initiating double contact) and the trailing arm is the arm holding the first handhold (ending double contact at release).

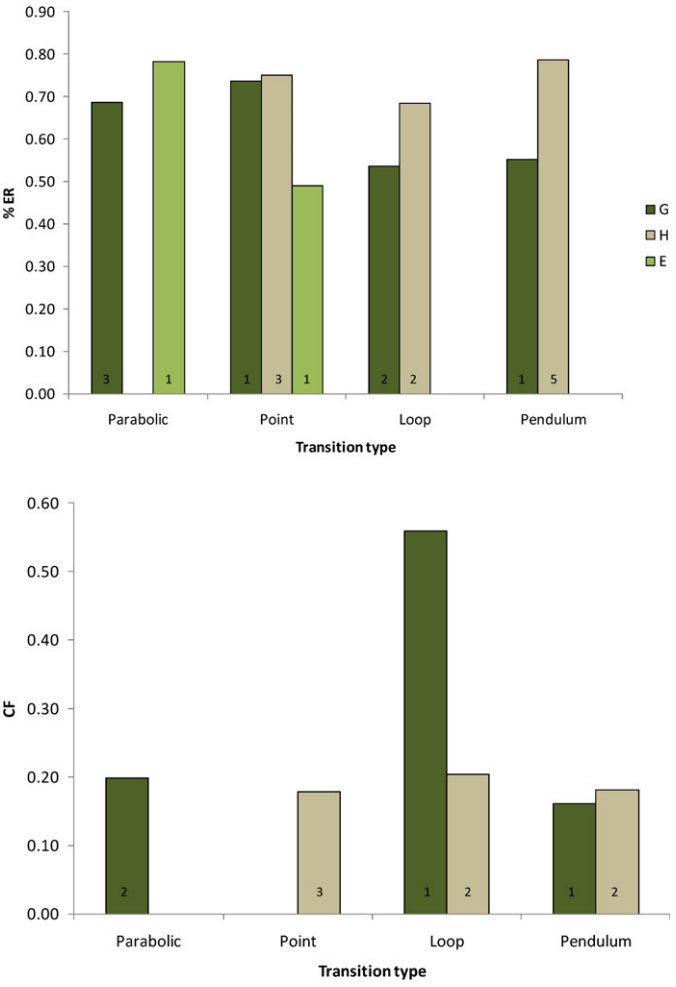

Fig. 5. Energy recovery and collision fraction as estimators of external work compared between transition types and individuals. Numbers in the boxes depict the number of sequences used for analysis. G, H and E are the three individual animals.

forces, is partly refuted. Forelimb joint angles during the swing phases of the strides characterized by different transition types are very similar, no clear differences in reaction force pattern is found and maximal vertical reaction forces do not differ.

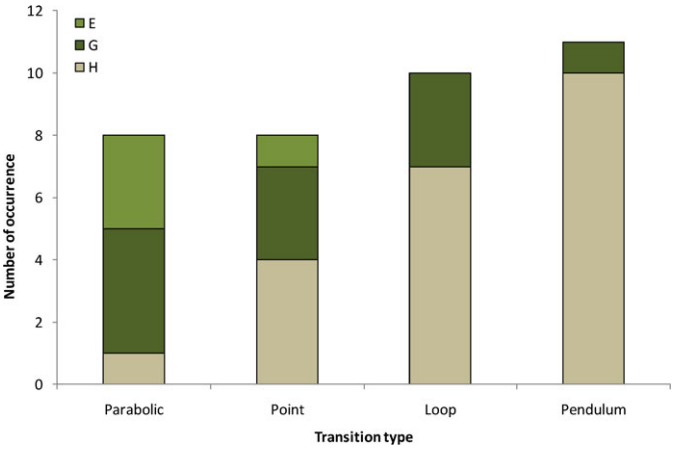

Fig. 6. Occurrence of each transition type in each individual G, H and E.

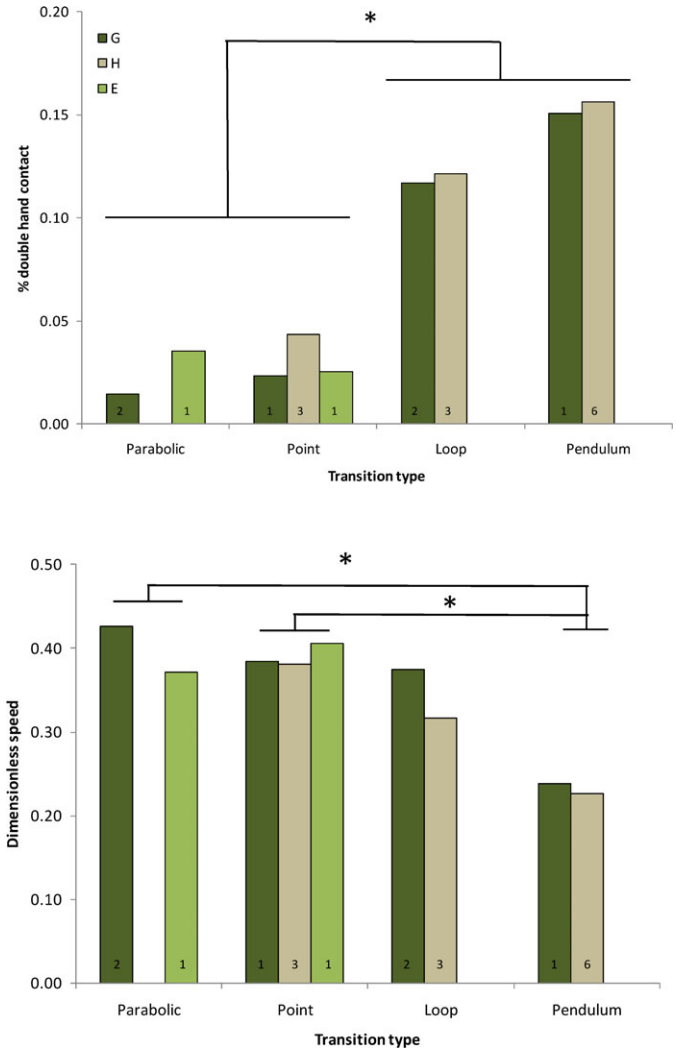

Fig. 7. Percentage of double hand contact and speed compared between transition types and individuals G, H and E. Numbers in the boxes depict the number of sequences used for analysis. Asterisks show significant differences between transition types.

However, joint angles and reaction forces during the double hand contact phase, do show characteristic differences (although this was not tested statistically).

The second hypothesis, i.e. that brachiation strides with different step-to-step transitions differ in efficiency, is refuted. ER and CF do not differ between the strides with different transition types.

Hypotheses three and four, are accepted. Individual preference for specific transition types is found and the transition types are used at different speeds.

When studying Figs 3 and 4, velocities, joint angles and reaction force profiles are very similar between strides with different transition types, at least during the swing phases (single contact). However, when interpreting the double hand contact phases, small, yet determinative, differences can be noticed. Differences in the shoulder and elbow angles of the trailing arm during double hand contact are most determinative, leading to different bCOM patterns associated with the different step-to-step transition types. Pendular and loop transitions can be

distinguished by the trailing elbow that flexes (loop transition) or remains extended (pendular transition). The flexing of the trailing arm elbow during the loop transition induces a lift of the bCOM and the trailing arm releases the handhold when the bCOM is at its highest point. This lifting of the bCOM can contribute to the pendular momentum, especially combined with release timing of the trailing hand at the highest point. Turnquist et al. (Turnquist et al., 1999) also observed this lifting of the bCOM by trailing elbow flexion during brachiation of woolley monkeys (*Lagothrix lagotricha)*, while spider monkeys (*Ateles fusciceps)* attain the same by using their tail (Turnquist et al., 1999). Jungers and Stern (Jungers and Stern, 1981) also described trailing elbow flexion in gibbon brachiation, although without indicating whether this was associated with a loop transition.

In point transitions, flexion of the trailing elbow was observed in our siamangs, but with a near constant trailing shoulder angle resulting in no extra lifting of the bCOM, because the body is already at its highest when grabbing the next support. Both shoulder and elbow angles of the leading arm remain the same during the double support phase and the swing phase in the point transition, indicating that double support phase is initiated with near ideal geometric conditions for the next swing. Whereas, in the pendular and loop transitions, the leading arm needs considerable extending before releasing the trailing hand.

Another explanation for the trailing arm bend is given by Usherwood and Bertram (Usherwood and Bertram, 2003). They explain it as a way to reduce energetic losses due to collisions, because it allows the bCOM path to be connected to the second swing path at a slow velocity and with a more favourable angle. We will come back to this point later in the discussion.

The parabolic transition seems different in the fact that both shoulder and elbow angles of the trailing arm remain the same and only the leading shoulder angle decreases slightly. Yet, the bCOM rises further during double hand contact and the trailing hand is released at the highest point. It seems in this case that the lift of the bCOM is not a consequence of a pulling action of the trailing arm, but it may be an inertia effect, because the vertical bCOM velocity is still relatively high at the beginning of double hand contact. Since substrate reaction forces are low (less than 20 N), the parabolic transition could be seen as a flight phase, though with two hands in contact with the handholds. With the leading hand already on the handhold, though without exerting any significant force, siamangs can easily optimize their timing of grabbing the next handhold, i.e. initiating the next swing from the highest point possible.

The occurrence of these differences in trailing and leading arm joint angles seem induced by the locomotor speed, both in terms of dimensionless speed as well as in the percentage of double hand contact. When an animal brachiates faster, the percentage of double hand contact decreases and it is more likely that a point or parabolic transition occurs while joint angles only change slightly. At slow speeds and high double contact percentages, the transition becomes a loop pattern or a reversed pendulum, with noticeable decreasing joint angles of the trailing arm and increasing joint angles of the leading arm. Chang et al. (Chang et al., 1997) already described such a loop transition, where the bCOM moves backwards during the double support phase (they found this for a white-handed gibbon, brachiating at 0.8 m/s, which concurs with the average velocity during which loop transitions occur in our measurements, i.e. 0.87 m/s). Their explanation for the occurrence of the loop pattern is that the handholds are placed closer together than optimal for their animal. In our case, however, each transition type occurred in setups with handholds either 0.8 or 1.2 m apart and the loop transition was used by the largest as well as the smallest individual. Therefore, we suggest that it is speed that determines which transition type is used and not step length, although some individual preference remains.

An additional contributing factor for changing transition types is peak force. Peak force is suggested to trigger gait change in various mammals (Biewener and Taylor, 1986; Farley and Taylor, 1991) and therefore, may be a determinant for the different transition types. Yet, although the vertical peak force increases with speed, no general difference in relative vertical maximal force is found between transition types. Although, the loop transition (second slowest) statistically has the highest vertical peak force, this is probably due to one relatively fast CCB sequence with a loop transition resulting in a high vertical peak force (and a high CF). So peak force may be kept constant by using the different step-to-step transition types in strides with different speeds.

Interesting to note is that our post hoc tests show that the significance of the differences in the percentage of double contact usually skips a transition type: e.g. parabolic differs from loop and pendulum, but not from point. Also, personal observations showed that, occasionally, intermediate bCOM patterns occur (e.g. a backward pendulum with a loop at each change of direction). Because of these observations we suggest there is a continuum overarching the predefined categories and the different CCB transition types are merely variations on the CCB gait connected to specific speeds.

Additionally, it could be questioned whether ricochetal brachiation is a dynamically different gait type from CCB, as ricochetal brachiation would fit in well as a parabolic transition at a higher speed, inducing a flight phase. Similarly to a running gait that cannot be determined solely on the duty factor being smaller than 0.5 (Biknevicius and Reilly, 2006), it seems hard to regard ricochetal brachiation as a distinct gait type, solely based on the existence of a flight phase.

The parabolic transitions from our dataset show duty factors between 0.47 and 0.59, but because there is no actual flight phase, they are considered CCB. Thus, the parabolic step-to-step transition, characteristic for ricochet, can occur during CCB as well. Moreover, no clear shift in locomotor mechanism is found. In our previous paper (Michilsens et al., 2011), we showed that ER is also determined by dimensionless speed and not by gait type. Even ricochetal brachiation has a significant amount of ER (58% on average) (Michilsens et al., 2011) indicating pendular mechanisms are present.

In contrast, Bertram et al. (Bertram et al., 1999) described ricochetal brachiation more as a bouncing gait instead of a pendulum driven mechanism and, in a later publication, Bertram and Chang (Bertram and Chang, 2001) described a whip-like transfer of rotational and translational kinetic energy in fast ricochetal brachiation that would drive the locomotion. Nevertheless, we never observed the characteristics of this whip-like transfer (i.e. a V-shaped bCOM pattern, drop in kinetic energy in mid-support). From our data it seems that if two dynamically distinct brachiation gaits exist, the transition is made at higher velocities than measured in our study and not at a duty factor of 0.5 as would be expected.

While different step-to-step transitions are used at different speeds and a higher speed may induce a lower ER (Michilsens et al., 2011), interestingly, no difference is found in efficiency between the brachiation strides with different transition types. Both measures used (ER and CF) show no difference between the strides with different transition types, regardless of the very different bCOM patterns involved. The fact that ER does not decrease at higher speeds between the different CCB transition types may be explained by the small speed range of CCB. When plotting the CCB data used in this paper on the general brachiation data of our previous paper (Michilsens et al., 2011), it can be seen that all data points have a low speed (Fig. 8). The ER referring to the pendulum theory (Cavagna et al., 1976; Preuschoft and Demes, 1984) stays relatively high with an average recovery rate of 70% (± 11.4%). Bertram and Chang (Bertram and Chang, 2001) found comparable results in brachiating white-handed gibbons (67.4%±18.4% at 1.2 m handhold spacing and 57.7%±14.0% at 0.8 m handhold spacing).

Alternatively, the relatively constant ER could also indicate that within CCB it is possible to keep the ER high by changing step-to-step transition type. As seen above, the adjusting of the bCOM during the double hand contact is primarily done by flexing of the trailing arm and extending of the leading arm at the right time. So, although the ER is relatively high, considerable internal work may be necessary to maintain this ER. Nevertheless, this is a rather efficient energy exchange rate compared to the ER in human walking (maximum of 65%) (Cavagna et al., 1976) and dogs walking (maximum of 70% at moderate speeds) (Griffin et al., 2004). Compared to gibbon bipedalism, with an ER of less than 25% (Vereecke et al., 2006), brachiation seems a very energy efficient locomotor mode (at least in terms of ER). Additionally, the same internal work necessary to adjust the bCOM, not only keeps the ER high, it also seems to improve the geometric conditions to avoid collisions while brachiating from one handhold to the other. This is demonstrated by the CF of 0.2 (±0.13), which points to a high amount of collision reduction and little energy loss. Only walking dogs approach this low collision fraction (0.26±0.08) (Lee et al., 2011). Walking goats, trotting and galloping dogs and goats have CFs of 0.48 up to 0.97, allowing many more collisional losses to occur (Lee et al., 2011). Considering this is a very new approach to determine collisional losses, comparative data are limited, yet a reduction of 80% of the possible collisional losses, is certainly high and it is the highest published value to date. Interestingly, several ricochetal collisionless theoretical models, where the release angle is the determining factor, have been formulated (Gomes and Ruina, 2005). From these, the most simple ones look like gibbon brachiation with a parabolic flight phase, though they also found a collisionless ricochetal loop transition. Obviously, during CCB other factors than the release angle can influence the collision geometry, such as the changing of the trailing and leading arm angles with the right timing (Usherwood and Bertram, 2003). Since no difference in CF between strides with different transition types is found, it seems that the trailing elbow flexion (during point and loop transitions) and the decreasing of the shoulder angle (in pendular and loop transitions) are factors that further help in avoiding the collisional losses of grabbing the next handhold with a less ideal angle. The importance of reduction of collisional losses in brachiation was made clear by Bertram et al. (Bertram et al., 1999), who based the predictions of his model on the minimizing of collisional losses and stated that the gibbon's behaviour matched the model and minimizes collisional losses (Bertram, 2004). Collisions and coinciding energy losses mainly occur during step to step transitions, which makes these transitions an important part of total locomotor costs. It is remarkable that during CCB four different step to step transition types occur, each of which minimize collisional losses.

Conclusion

In conclusion, it can be said that siamang continuous contact brachiation dynamics can be explained by both the pendulum model and the collision reduction theory. Brachiation strides with four step-to-step transition types are observed, all of which have

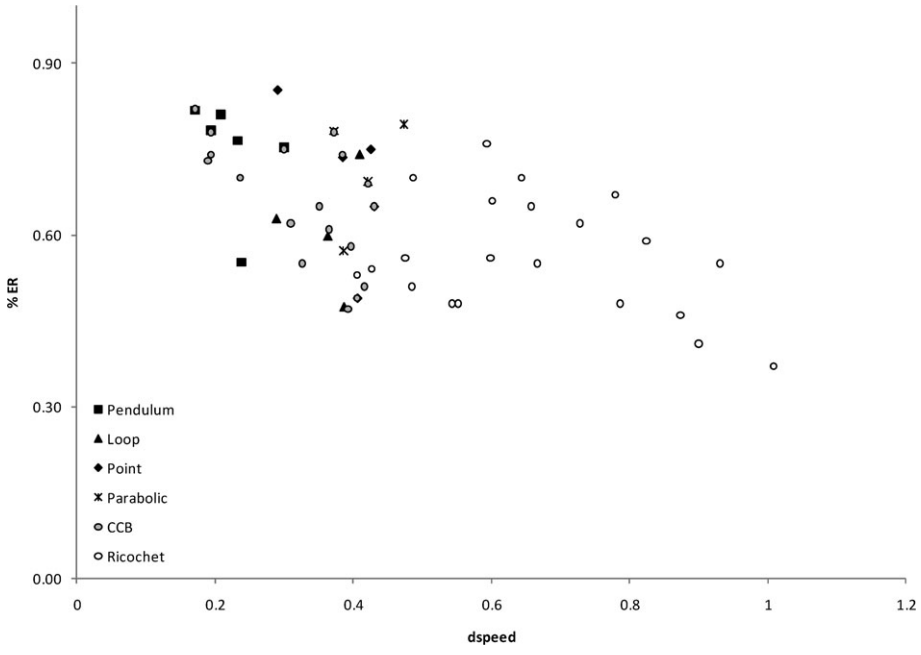

Fig. 8. Energy recovery during one stride relative to dimensionless speed. (Adapted from a previous publication) (Michilsens et al., 2011). Different marker shapes indicate the different transition types; circles indicate data taken from a previous publication (Michilsens et al., 2011), which include continuous contact brachiation (CCB; filled circles) and ricochetal brachiation (open circles) strides.

high energy recoveries and low collision fractions. Variability in step-to-step transitions seem to occur to keep an equally efficient use of external work at different brachiation speeds. Transition types are only associated with speed, which affects the percentage of double hand contact and relative maximal vertical force. However, as intermediate forms may occur, these transition types form a continuum, rather than clearly distinct types, and may even give rise to a flight phase (and thus ricochet) when speed increases further.

Acknowledgements

I would like to thank the students who helped with collecting the data and Arne Iserbyt for statistical help. I also thank the Zoo keepers for making it possible for me to collect data whenever possible. Jan Scholliers I thank for his help in developing the setup and Josie Meaney-Ward for English linguistic advice. Thanks to the anonymous referees for their helpful comments on the original manuscript. This study was supported by a research grant to the first author from the Research Foundation Flanders (FWO) and by structural support to the Centre for Research and Conservation by the Flemish Government.

Competing Interests

The authors declare that there are no competing interests.

References

Bertram, J. E. (2004). New perspectives on brachiation mechanics. *Am. J. Phys. Anthropol*. **125**, **Suppl 39**, 100-117.

Bertram, J. E. and Chang, Y. H. (2001). Mechanical energy oscillations of two brachiation gaits: measurement and simulation. *Am. J. Phys. Anthropol.* **115**, 319-326.

Bertram, J. E., Ruina, A., Cannon, C. E., Chang, H. Y. and Coleman, M. J. (1999). A point-mass model of gibbon locomotion. *J. Exp. Biol.* **202**, 2609-2617.

Biewener, A. A. and Taylor, C. R. (1986). Bone strain: A determinant of gait and speed. *J. Exp. Biol.* **123**, 383-400.

Biknevicius, A. R. and Reilly, S. M. (2006). Correlation of symmetrical gaits and whole body mechanics: Debunking myths in locomotor biodynamics. *J. Exp. Zool.* **305A**, 923-934.

Cavagna, G. A., Thys, H. and Zamboni, A. (1976). The sources of external work in level walking and running. *J. Physiol.* **262**, 639-657.

Chang, H. Y., Bertram, J. E. and Ruina, A. (1997). A dynamic force and moment analysis system for brachiation. *J. Exp. Biol.* **200**, 3013-3020.

Farley, C. T. and Taylor, C. R. (1991). A mechanical trigger for the trot-gallop transition in horses. *Science* **253**, 306-308.

Fleagle, J. G. (1976). Locomotion and posture of the Malayan siamang and implications for hominid evolution. *Folia Primatol. (Basel)* **26**, 245-269.

Gomes, M. W. and Ruina, A. L. (2005). A five-link 2D brachiating ape model with life-like zero-energy-cost motions. *J. Theor. Biol.* **237**, 265-278.

Griffin, T. M., Main, R. P. and Farley, C. T. (2004). Biomechanics of quadrupedal walking: how do four-legged animals achieve inverted pendulum-like movements? *J. Exp. Biol.* **207**, 3545-3558.

Jungers, W. L. and Stern, J. T., Jr. (1981). Preliminary electromyographical analysis of brachiation in gibbon and spider monkey. *Int. J. Primatol.* **2**, 19-33.

Lee, D. V., Bertram, J. E., Anttonen, J. T., Ros, I. G., Harris, S. L. and Biewener, A. A. (2011). A collisional perspective on quadrupedal gait dynamics. *J. R. Soc. Interface* **8**,1480-1486.

Michilsens, F., Vereecke, E. E., D'Août, K. and Aerts, P. (2009). Functional anatomy of the gibbon forelimb: adaptations to a brachiating lifestyle. *J. Anat.* **215**, 335-354.

Michilsens, F., D'Août, K. and Aerts, P. (2011). How pendulum-like are siamangs? Energy exchange during brachiation. *Am. J. Phys. Anthropol.* **154**, 581-591.

Preuschoft, H. and Demes, B. (1984). Biomechanics of brachiation. In *The Lesser Apes: Evolutionary And Behavioral Biology* (H. Preuschoft, D. J. Chivers, W. Y. Brockelman and N. Creel) 96-118.Edinburgh: Edinburgh University Press.

Turnquist, J. E., Schmitt, D., Rose, M. D. and Cant, J. G. (1999). Pendular motion in the brachiation of captive *Lagothrix* and *Ateles*. *Am. J. Primatol.* **48**, 263-281.

Usherwood, J. R. and Bertram, J. E. (2003). Understanding brachiation: insight from a collisional perspective. *J. Exp. Biol.* **206**, 1631-1642.

Vaughan, C. L. and O'Malley, M. J. (2005). Froude and the contribution of naval architecture to our understanding of bipedal locomotion. *Gait Posture* **21**, 350-362.

Vereecke, E. E., D'Août, K. and Aerts, P. (2006). The dynamics of hylobatid bipedalism: evidence for an energy-saving mechanism? *J. Exp. Biol.* **209**, 2829-2838.